Real-time X-ray-based 4D image guidance of minimally invasive interventions

Jan Kuntz, Rajiv Gupta, Stefan O. Schönberg, Wolfhard Semmler, Marc Kachelrieß & Sönke Bartling

European Radiology

ISSN 0938-7994
Volume 23
Number 6

Eur Radiol (2013) 23:1669-1677
DOI 10.1007/s00330-012-2761-2

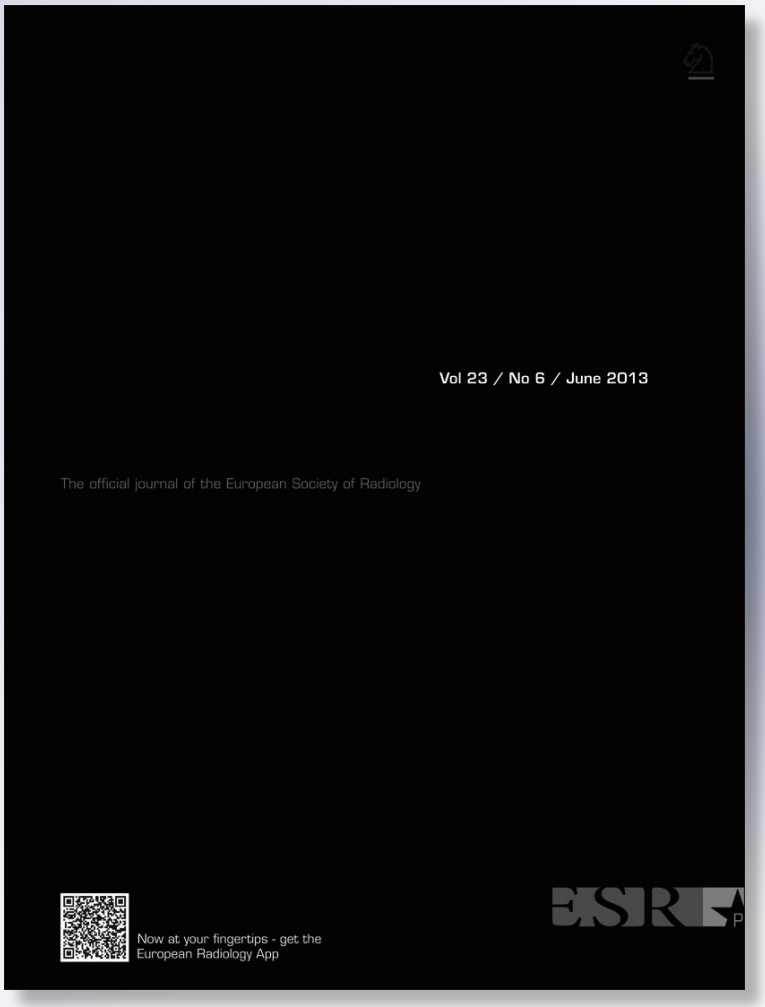

Springer

Eur Radiol (2013) 23:1669–1677
DOI 10.1007/s00330-012-2761-2

INTERVENTIONAL

Real-time X-ray-based 4D image guidance of minimally invasive interventions

Jan Kuntz · Rajiv Gupta · Stefan O. Schönberg · Wolfhard Semmler · Marc Kachelrieß · Sönke Bartling

Received: 20 August 2012 / Revised: 24 November 2012 / Accepted: 28 November 2012 / Published online: 12 January 2013

Abstract
Objective A new technology is introduced that enables real-time 4D (three spatial dimensions plus time) X-ray guidance for vascular catheter interventions with acceptable levels of ionising radiation.
Methods The enabling technology is a combination of low-dose tomographic data acquisition with novel compressed sensing reconstruction and use of prior image information. It was implemented in a prototype set-up consisting of a gantry-based flat detector system. In pigs ($n=5$) angiographic interventions were simulated. Radiation dosage on a per time base was compared with the "gold standard" of X-ray projection imaging.
Results Contrary to current image guidance methods that lack permanent 4D updates, the spatial position of interventional instruments could be resolved in continuous, spatial 4D guidance; the movement of the guide wire as well as the expansion of stents could be precisely tracked in 3D angiographic road maps. Dose rate was 23.8 μGy/s, similar to biplane standard angiographic fluoroscopy, which has a dose rate of 20.6 μGy/s.
Conclusion Real-time 4D X-ray image-guidance with acceptable levels of radiation has great potential to significantly influence the field of minimally invasive medicine by allowing faster and safer interventions and by enabling novel, much more complex procedures for vascular and oncological minimally invasive therapy.
Key Points
- *Real-time 4D (three spatial dimensions plus time) angiographic intervention guidance is realistic.*
- *Low-dose tomographic data acquisition with special compressed sensing-based algorithms is enabled.*
- *Compared with 4D CT fluoroscopy, this method reduces radiation to acceptable levels.*
- *Once implemented, vascular interventions may become safer and faster.*
- *More complex intervention approaches may be developed.*

Keywords Intervention guidance · 4D imaging · Compressed sensing · Catheter lab · Minimally invasive

Electronic supplementary material The online version of this article (doi:10.1007/s00330-012-2761-2) contains supplementary material, which is available to authorized users.

J. Kuntz · W. Semmler · M. Kachelrieß · S. Bartling (✉)
Department of Medical Physics in Radiology,
German Cancer Research Center—DKFZ, Im Neuenheimer Feld 280,
69120 Heidelberg, Germany
e-mail: soenkebartling@gmx.de

J. Kuntz
e-mail: j.kuntz@dkfz.de

W. Semmler
e-mail: semmler.office@dkfz.de

M. Kachelrieß
e-mail: marc.kachelriess@dkfz.de

R. Gupta
Department of Radiology, Harvard Medical School,
Massachusetts General Hospital, 55 Fruit St, FND 2,
Boston, MA 02114, USA
e-mail: rgupta1@partners.org

S. O. Schönberg · S. Bartling
Institute of Clinical Radiology and Nuclear Medicine,
Medical Faculty Mannheim, Heidelberg University,
Theodor-Kutzer-Ufer 1-3,
68167 Mannheim, Germany
e-mail: stefan.schoenberg@umm.de

Introduction

Image-guided radiological and cardiological interventions play an ever-growing role in the field of minimally invasive medicine. Of all these minimally invasive procedures,

intravascular interventions are foremost. Cardiovascular treatments and tumour embolisation therapies also play a major role in health care.

The scope of interventional radiology is broad and, as procedures become more complex, the requirements for professional training increase. The demands are such that it is likely that there will be a translational gap between the theoretical availability and actual implementation of advanced procedures such as transcatheter aortic valve replacement (TAVI) [1] and aortic endovascular stent grafting. For this reason, it will be necessary to develop and introduce new and enabling image guidance methods.

Despite radiation exposure, X-ray-based guidance methods are those most commonly used for image-guided minimally invasive medicine. Other guidance methods are limited because of technical and engineering constraints. For example, ultrasound guidance is limited by penetration depth in tissue and magnetic resonance imaging (MRI) guidance is limited by the detectability of interventional instruments, image resolution and limited patient access because of the strong magnetic field [2, 3].

Practical real-time 4D imaging (three spatial dimensions plus time) that would allow continuous spatial display of interventional instruments and their surroundings has not yet been realised. Current X-ray-based interventional guidance techniques leave the interventionalist with considerable uncertainty about the spatial position of instruments and their relation to the underlying anatomy. Usually, spatial positioning depends on time-resolved two-dimensional (2D) projection imaging alone, which may be supported by occasional 3D information derived from an angiographic computed tomography (CT) [4]. In CT-guided interventions, continuous guidance is omitted and the interventionalist relies on technological rather than tactile feedback while moving instruments in between CT acquisitions [5]. The drive to overcome the limitations associated with current methods can be demonstrated by the considerable efforts that have been made in the past to combine imaging with instrument navigation set-ups [6, 7]and to co-register 3D imaging such as CT or MRI with X-ray fluoroscopy [8, 9].

Continuous CT data acquisition, which technically produces 4D data sets, would result in unacceptably high doses of ionising radiation to the patient as well as to the interventionalists [10]. Therefore, up until now, no continuous 4D guidance method has been available that operates within tolerable radiation doses comparable to the current "gold standard" of interventional radiology, X-ray fluoroscopy.

We have developed a new method that can produce 4D data sets at an acceptable radiation dose by incorporating a novel theorem into image reconstruction, the *compressed sensing* (CS) theory. We have found that useful tomographic images can be reconstructed even if the data are highly undersampled and violate the Shannon–Nyquist theorem. CS has evolved slowly over the last decade, but was finally mathematically proven to deliver accurate results [11] and was recently introduced into medical imaging [4, 12–14]. CS is based on the concept that many signals are sparse, that is, they contain many coefficients close to or equal to zero when represented in an appropriate imaging domain; a constraint that can often be fulfilled directly or after applying a sparsifying function in medical imaging. CS can be implemented in tomographic reconstruction by solving the following l1-norm minimisation problem in an iterative process [12, 15]:

$$\min_X |\Psi X|_{l1}$$

subject to

$$\min_X |AX - Y|_{l2}^2$$

where X is the image to be determined, A is the system matrix describing the tomographic system's geometric and physical properties, and where Y indicates the projection data; Ψ is the sparsifying function, which must contain prior knowledge of the examined object, such as the fact that the gradient of the image is non-zero mainly in regions where edges are present, or from prior imaging data of the same object [16].

In 4D interventional guidance, several constraints are applicable that comply well with the CS theorem. Changes to the examined volume that are caused by interventional instruments such as guide wires, catheters, biopsy needles and stent struts are sparse in image representation (Fig. 1). Thus a comparison with a prior image data set (e.g. before interventional instruments are inserted) sparsifies data from low-dose updated CT images that are continuously acquired during intervention. Usually temporal changes are small. CS theory relates the degree of change to the amount of sampling data, hence the radiation dose. Therefore, only a relatively small dose of radiation is sufficient to update information. These changes can be incorporated into the prior dataset using iterative CS algorithms [16]. Additional constraints can be used to reduce the radiation dose needed for 4D interventional guidance, including the predominance of high-contrast structures, the low relevance of absolute Hounsfield units and a certain tolerance to imaging artefacts.

The aim of this study is to show by means of a prototype set-up, including animal experiments, that 4D interventional guidance as well as 3D road mapping with acceptable radiation dose levels is possible using the techniques developed here.

Materials and methods

To fulfil this aim a prototype set-up that is able to simulate 4D intervention guidance was built, compressed sensing algorithms implemented and interventions were performed on

pigs. The underlying concept for 4D intervention guidance was to combine information from an initial full-dose prior CT examination with continuously acquired low-dose updates in a compressed sensing reconstruction (Fig 1). Furthermore a road map that shows the vascular anatomy is necessary for interventional guidance. While 2D road maps are sufficient for projective interventional guidance, 3D road maps should be generated to exploit the full advantages of spatial guidance in 4D interventional procedures. Therefore, low-dose CT updates after contrast medium injection was also combined with the information from the initial prior CT examination and the vascular road map used for 3D road mapping.

Necessary radiation doses were compared with the radiation dose that is currently needed for intervention guidance using an internal standard that was imaged in our prototype as well as the current state-of-the-art X-ray fluoroscopy set-up.

Flat-detector CT system

The core of the experimental set-up was a flat-detector-based imaging system with components that resemble current imaging chains within interventional guidance C-arm systems. Contrary to C-arm-based imaging chains, it was mounted on a continuously rotating gantry [17]. The flat-detector cone-beam CT system allows the imaging of a volume of 250×250×180 mm^3, which represents the volume of interest for neuroradiological interventions and numerous cardiac settings. The CsI/amorphous silicon flat detector (PaxScan 4030CB; Varian Medical Systems, Mountain View, CA) can be operated at a read-out rate of 30 fps in a 2×2 pixel binning mode, resulting in an effective pixel size of 260×260 μm^2 in the iso-centre. The X-ray tube current can be varied from 2 to 50 mA with a voltage range of 80–140 kV, while the focal spot size is about 400 μm.

Vascular interventions

While continuous projection data were acquired, vascular interventions were performed in five 4-month-old pigs with an average weight of 38 kg and a range of 30–50 kg. Standard arterial vascular access systems were placed in the common carotid arteries (e.g. Radiofocus Introducer II,

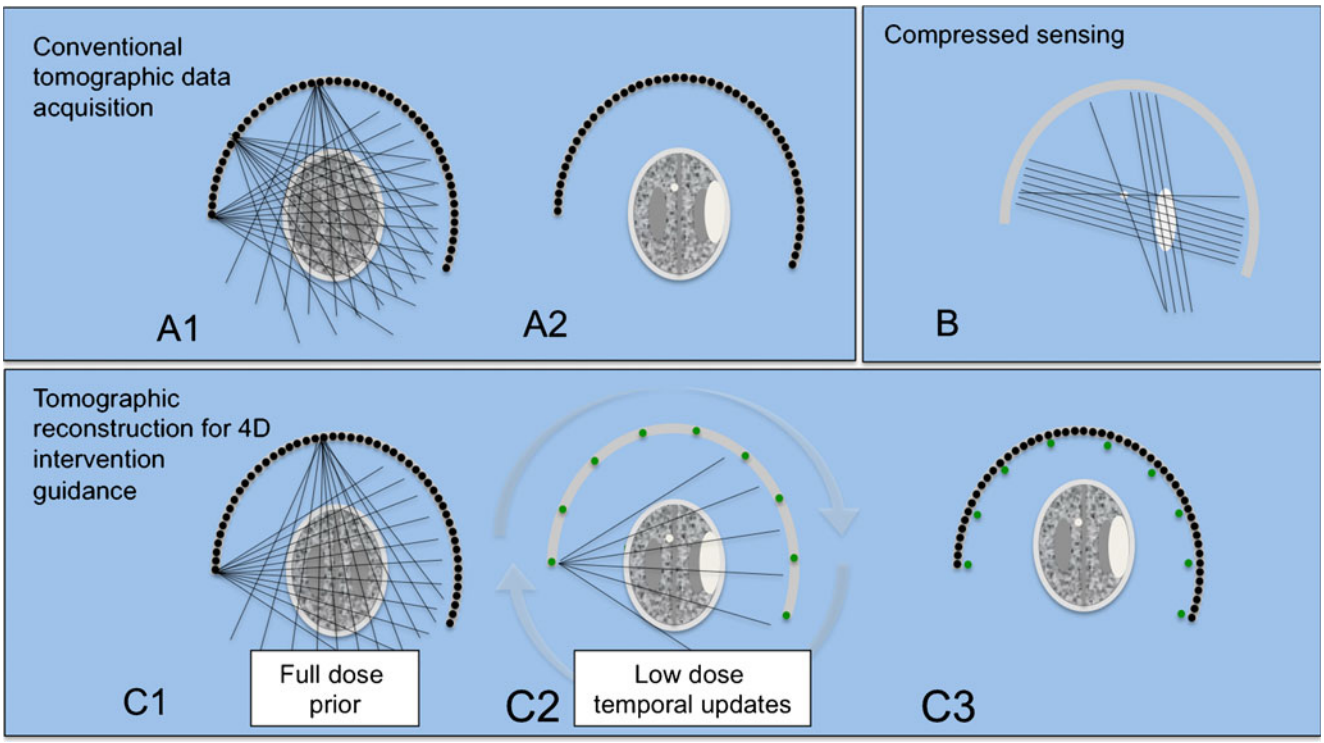

Fig 1 In conventional tomographic data acquisition, full projection data sets are acquired and reconstructed using standard back-projection techniques (**a1**). This is also done in repeated acquisitions of the same volume, e.g. for several time points during interventions (**a2**, *white inserts* resemble changing structures in the head such as an introduced catheter tip, stent or contrast media). Here, full radiation dose data sets are always acquired despite the fact that changes in the volume are sparse. Those sparse changes could be reconstructed from very few data points (and hence with very low radiation dose) by minimising the l1 norm as demonstrated in the compressed sensing (CS) theory (**b**). We propose CS as the enabling concept for practical 4D intervention guidance, as demonstrated here. After acquiring a full-dose prior CT data set (**c1**), low-dose temporal updates are continuously imaged with a limited number of projections (**c2**). The updates are incorporated into the prior CT data using an iterative, CS-based algorithm (**c3**) to yield images of a similar quality to standard CTs (**a2**) but with only a fraction of the radiation dose

Fr 9 [Terumo, Tokyo, Japan]) or femoral arteries (e.g. Flexor Shuttle Select, Tuohy-Borst Side-Arm Introducer [William Cook Europe, Bjaeverskov, Denmark]). Catheters (e.g. Radiofocus Angiographic Catheter, Femoral-Cerebral Headhunter, Fr 5 and Radiofocus Glidecath, Simmons/Sidewinder 2 Fr 4 [Terumo, Tokyo, Japan]) or guide wires (e.g. Radiofocus guide wire, 0.89 mm diameter, 150 cm length, angled [Termuo, Tokyo, Japan]) were used for the simulation of interventional procedures. Three self-expanding stents (one Misago, 7 mm in diameter, 80 mm long [Terumo, Tokyo, Japan] and two Wallstent-Uni, 12 mm in diameter, 4 cm long [Boston Scientific, Boston, MA, USA]) were expanded in the carotid artery.

All animal experiments conducted in this study were performed in strict accordance with the local recommendations for the handling of laboratory animals. The protocol (AZ 35–9185.81/L2-6/06) was approved by the local committee on the Ethics of Animal Experiments of the Regierungspräsidium of the federal state Baden-Württemberg, Germany. All interventions were performed under ketamine, midazolam and azaperone anaesthesia and the experiments resulted in euthanasia within narcosis.

4D interventional guidance

A standard CT examination (80 kV, 30 mA, 19 s full imaging time, 30 fps) was acquired before the interventional procedure. No instruments were present during this initial CT examination. To provide a 3D vascular road map, contrast-enhanced acquisitions were performed with a 4 s rotation time and 20 s full imaging time, while a total of 20 ml contrast agent (Imeron 300; Bracco, Milan, Italy) was injected through an arterial catheter with a flow rate of 2 ml per second. Datasets were reconstructed using 16 projections, distributed over 180°.

During the continuous movement of interventional instruments, update image data were acquired (80 kV 30 mA, 4 s rotation time, 20 rotations, 30 fps, 120 projections per rotation, 3° projection increment). Selective acquisition of projections on predefined angular positions was not possible with our instrumentation. Therefore, undersampling was retrospectively simulated by discarding three out of four projections, resulting in a projection increment of 12° (15 projections) covering a half rotation, which is the minimum angular range to reconstruct an image. In addition, quantum noise was added to the projection images to simulate low-dose image acquisition. The full-dose prior image data set, together with the simulated undersampled, low-dose update image data with added noise, were reconstructed using several algorithms. Continuous 4D data sets were created by continuously sliding 180° data at 90° increments (temporally overlapping reconstructions). The 4D datasets were displayed and rated using standard post-processing software (Syngo Inspace; Siemens, Forchheim, Germany; ImageVis3D, Scientific Computing and Imaging Institute, The University of Utah, UT, USA).

Reconstruction algorithms

All image reconstructions were conducted on our C++−based framework. Standard, well-established non-iterative CT reconstruction algorithms such as those by Feldkamp–Davis–Kress (FDK) [18] and McKinnon–Bates (MKB) [19] were used to reconstruct the prior, fully sampled data sets as well as dose-reduced update data sets for comparison. Iterative CS algorithms, ASD-POCS (adaptive steepest descent–projections onto convex sets) [12] and PICCS (prior image constrained compressed sensing) [20] algorithms were used. In addition, a novel reconstruction algorithm called prior image dynamic interventional computed tomography (PRIDICT) was developed, taking several constraints of interventional guidance into account. During interventional guidance, the changes from a good quality initial CT are sparse even without a sparsifying transformation, such as total variation or other gradient functions. Compared with PICCS and ASD-POCS such sparsifiying function was omitted and only the difference to the prior image was used as sparsifying transform. The amount of acceptable changes in comparison with the prior data set was correlated according to the CS theory to $M/\ln N$ pixels, where M is the number of independent measurements (being the number of rays in the centre slice) and $N \times N$ is the size of the reconstruction matrix [21]. This concept was implemented within PRIDICT as follows. A standard FDK reconstruction of the prior image was performed, representing the static structures with high quality. Afterwards, the temporal information of the interventional instruments was incorporated in an iterative process, where the difference image from the forward projection of the current image and the update scan was reconstructed separately using a FDK algorithm with a soft kernel, while only the pixels with the highest absolute values were added to the current image, weighted to assure maximum improvements in raw data fidelity.

Dose comparison

In order to compare the applied radiation dose from biplane-fluoroscopy to the 4D interventional guidance, we placed a modified 160-mm (diameter) CT dose index (CTDI) head phantom [22] in a current C-arm system (Artis zee; Siemens Healthcare, Forchheim, Germany) and in the flat detector CT system. A dose profile at the centre bore of the CTDI phantom was measured with a 100 mm CT ionization chamber (type 30009; PTW Freiburg, Germany); the dose chamber was placed at five positions along the z-axis Standard intervention guidance imaging parameters were used (C-arm: FOV

250 mm×180 mm, 7.5 fps, automated exposure control; flat detector CT: FOV 250 mm×180 mm, 80 kV, 50 mA, 10 s rotation time, pulsation). Dose rates were calculated from measured air kerma [22, 23]. Acquired datasets were retrospectively undersampled (only every *n*-th projection was used) and the dose rates of 4D intervention guidance were corrected for this undersampling factor. Further dose reduction was simulated by adding quantum noise to projection images. Dose reduction factors for the additional noise in the projection images were determined from noise measurements in fully sampled reference reconstructions assuming that a dose reduction of 50 % will increase the noise in the reconstructed CT image by a factor of $\sqrt{2}$ [24].

Data analysis

Image quality was analysed by two experienced radiologists in consensus on an ordinal scale. Display of interventional instruments was rated as follows: 0, no instrument visible; 1, instrument visible, no structural information; 2, instrument visible, structural information (such as guide wire tip, stent struts), but artefacts visible; 3, guide wire fully visible and instrument structure visible on an artefact-free CT quality image. The visibility of the surrounding anatomy was rated as follows: 0, no surrounding anatomy visible; 1, rough, but blurred anatomy visible; 2, good visibility of surrounding anatomy.

Two board-certified radiologists, highly-experienced in radiological interventions, assessed the usability of reconstructions for interventional guidance.

Results

Angiographic interventions were successfully performed in full-sized pigs (n=5) while they underwent continuous

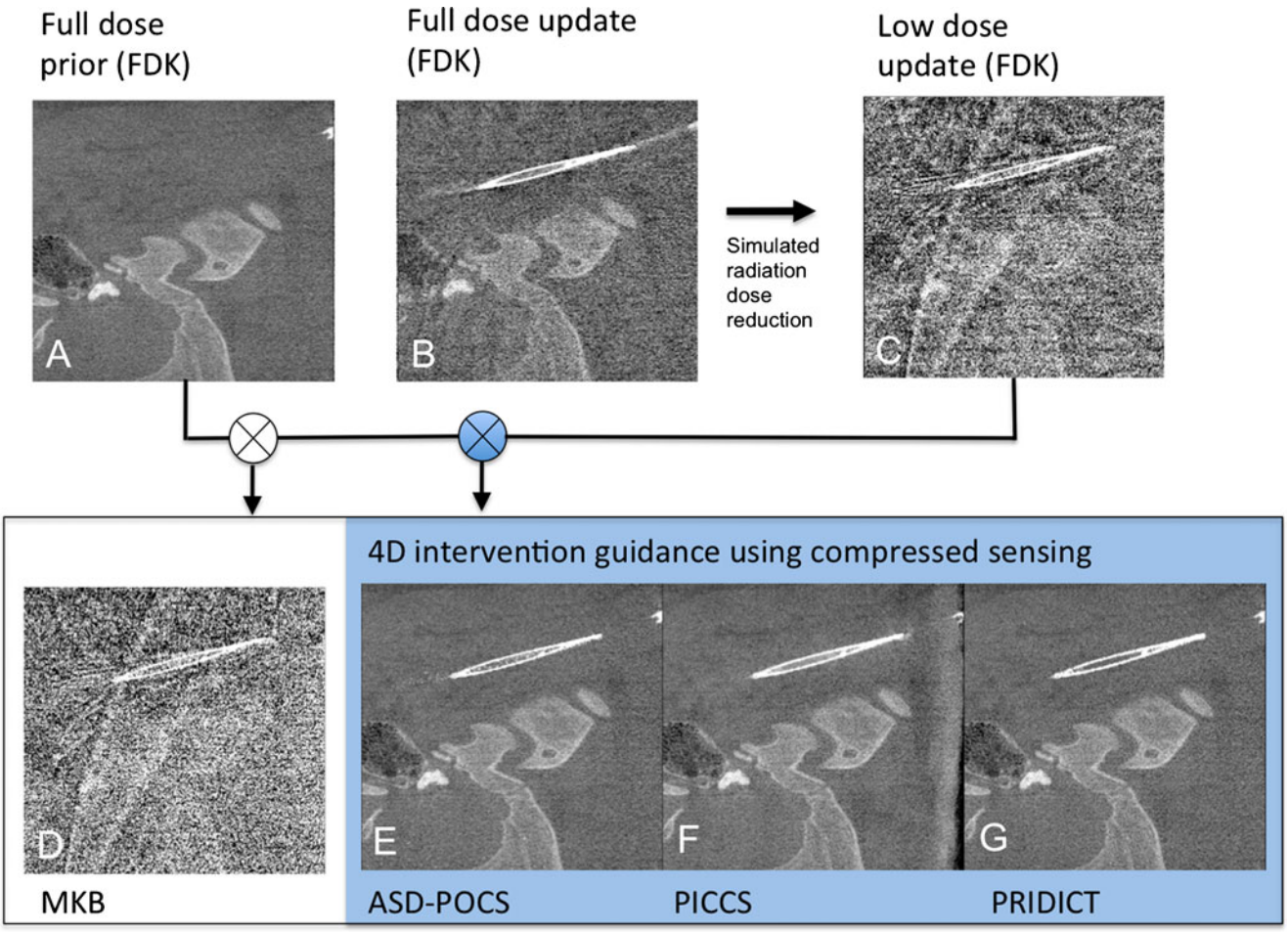

Fig 2 Four-dimensional interventional guidance with tomographic reconstruction, as demonstrated by the insertion of a stent into the carotid artery of a pig. A full-dose prior CT data set (**a**) was acquired before the stent was inserted into the carotid artery. **b** A full-dose update image (**b**) and update images from a simulated low radiation dose rate (dose rate twice that of standard fluoroscopy) with a limited number of projections, using standard CT reconstruction algorithms, FDK (**c**) and MKB (**d**) are shown respectively. Reconstruction of the same data using CS-based algorithms, ASD-POCS (**e**), PICCS (**f**) or PRIDICT (**g**), provides image quality that is comparable to that of a standard full-dose CT and that is sufficient for 3D intervention guidance

imaging in the aforementioned cone-beam CT system. Data were initially acquired in a standard high-dose CT setting (559.8 μGy/s, all air kerma). The number of projections was reduced and noise was added before reconstruction so that the corresponding dose rate was equivalent to an acquisition with a dose rate of 23.8 μGy/s, similar to biplane standard fluoroscopy, which has a dose rate of 20.6 μGy/s.

A full-dose head CT (9.7 mGy) was used to provide an initial prior dataset. Low-dose update data were continuously provided during intervention and, if these data were reconstructed with a standard CT reconstruction algorithm, image quality was poor. Similarly, a combination of prior data with low-dose update data reconstructed using a standard algorithm, MKB, yielded insufficient image quality. Only CS-based reconstructions were able to show interventional instruments and surrounding structures in an image of comparable quality equivalent to that of standard CT acquisitions (Fig. 2). PRIDICT, the algorithm that was especially designed for interventional guidance, resulted in the best display of interventional instruments (3 out of 3 rating points), whereas the ASD-POCS (2 rating points) as well as PICCS (2 rating points) algorithm resulted in sufficient image quality. All CS algorithms showed surrounding structures in best quality (3 out of 3 rating points).

As described above, a road map that shows the vascular anatomy is necessary for interventional guidance. While 2D road maps are sufficient for projective interventional guidance, 3D road maps should be generated to exploit the full advantages of spatial guidance in the 4D interventional procedure. Using standard angiographic CT techniques to obtain a 3D arterial vascular anatomy of the head would require an effective dose of 422 μSv in this set-up. In comparison, CS reconstruction that embodies prior data resulted in large dose savings. Here, sufficient image quality was achieved from 16 projections per update reconstruction, with a radiation dose of only 11 μSv. Vascular road maps were integrated into 4D interventional guidance.

In 4D interventional guidance data sets, interventional instruments could be traced in space with a sufficient time resolution of 16 updates per second, resulting in one unique dataset per second. We found that the positions of stents, guide wires and coils were clear with respect to the 3D

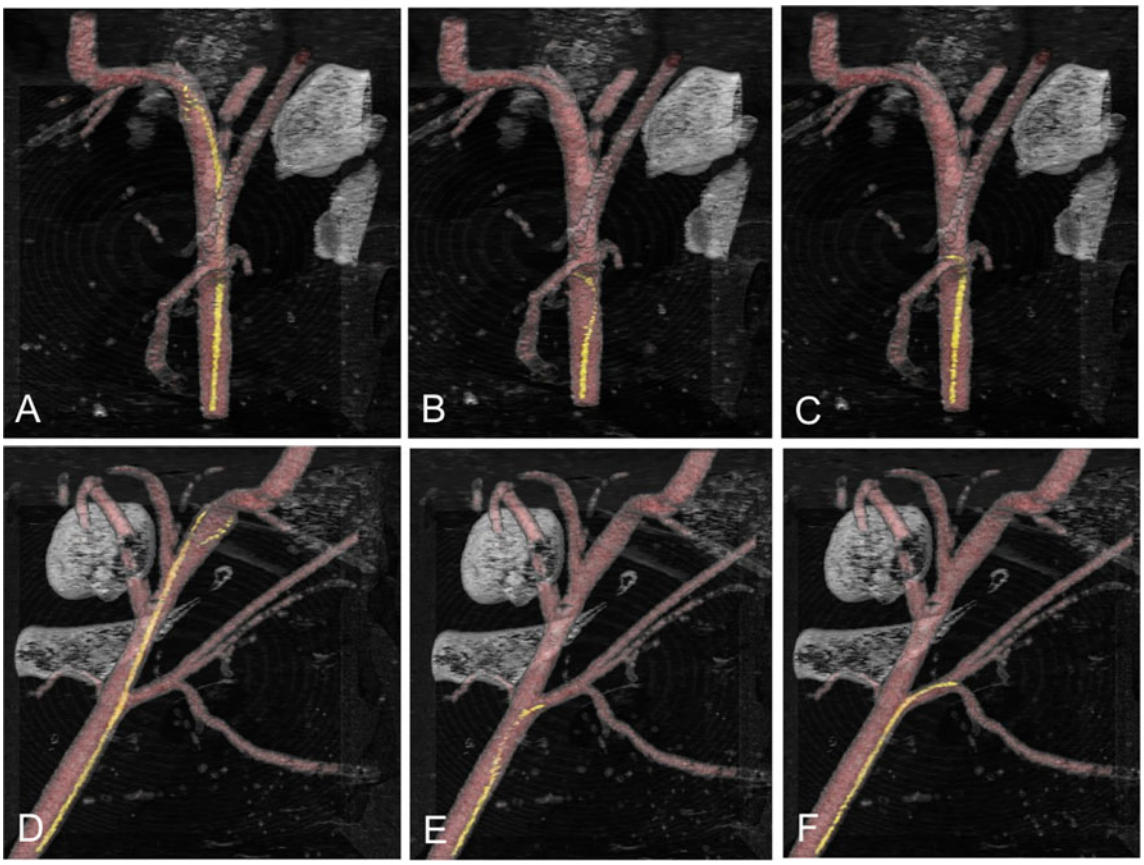

Fig 3 Colour-coded volume rendering of 4D interventional guidance of a guide wire in a pig. Anterior (**a-c**) and lateral views from the right (**d-f**) at three different time points are provided. The bent guide wire is visible in the external carotid artery (**a, d**), from which it was retracted into the common carotid artery (**b, e**), placed in front of the ostium of the ascending pharyngeal artery, and then advanced into that artery (**c, f**). At all times the spatial position of the guide wire as well as its tip was clear. (*See* Supplementary video 1)

vascular road map, as well as the surrounding soft-tissue and bone anatomy. Resolution was sufficient to show the tips of the instruments, such as the bend tip of a guide wire, which could be localised in space and followed into the ostium of upbranching vessels (Fig. 3, Supplementary video 1). The relationship of interventional instruments with respect to each other was clear. Stent positions could be precisely assessed and the spatial unfolding of stents could be visualised (Fig. 4, Supplementary video 2). Resulting data sets were considered sufficient for interventional guidance by radiologists.

Discussion

Contrary to common belief, we were able to prove that 4D interventional CT guidance is possible within acceptable radiation dose levels using the method described. The advantages of 4D imaging in minimally invasive interventions are multiple:

1. The spatial position of instruments is always clear.
2. Surrounding structures, such as vessels and other instruments, can be visualised.
3. Instruments can be moved much more precisely and can be target-orientated.
4. It avoids trial and error approaches that result in bidirectional movement of catheters past vessel ostia and the bent catheter tip can be visually directed towards the ostium.
5. Critical measurements that currently rely on pre-interventional CTs can be continuously verified intraprocedurally.

Consequently, accurate 4D information may lead to faster, more directed and safer image-guided interventions. In certain applications, the advantages could be even greater. For example, in aneurysm coiling where precise localisation of coils and stents into the base of the aneurysm is crucial, 4D interventional guidance could significantly improve the outcome. Precise localisation may also mean that more complex procedures can be devised and completely novel interventional procedures may become feasible.

In the future, even more dedicated 4D interventional guidance algorithms could be developed that allow the continuous acquisition and reconstruction of prior images during the interventional procedure that compensate for complex respiratory or cardiac motion and correct for patient motion [4]. Solutions to these challenges can be adopted from various fields of medical image processing.

In this study, real-time 4D imaging of interventional guidance was performed by simulating all necessary conditions. All 4D data sets were retrospectively reconstructed

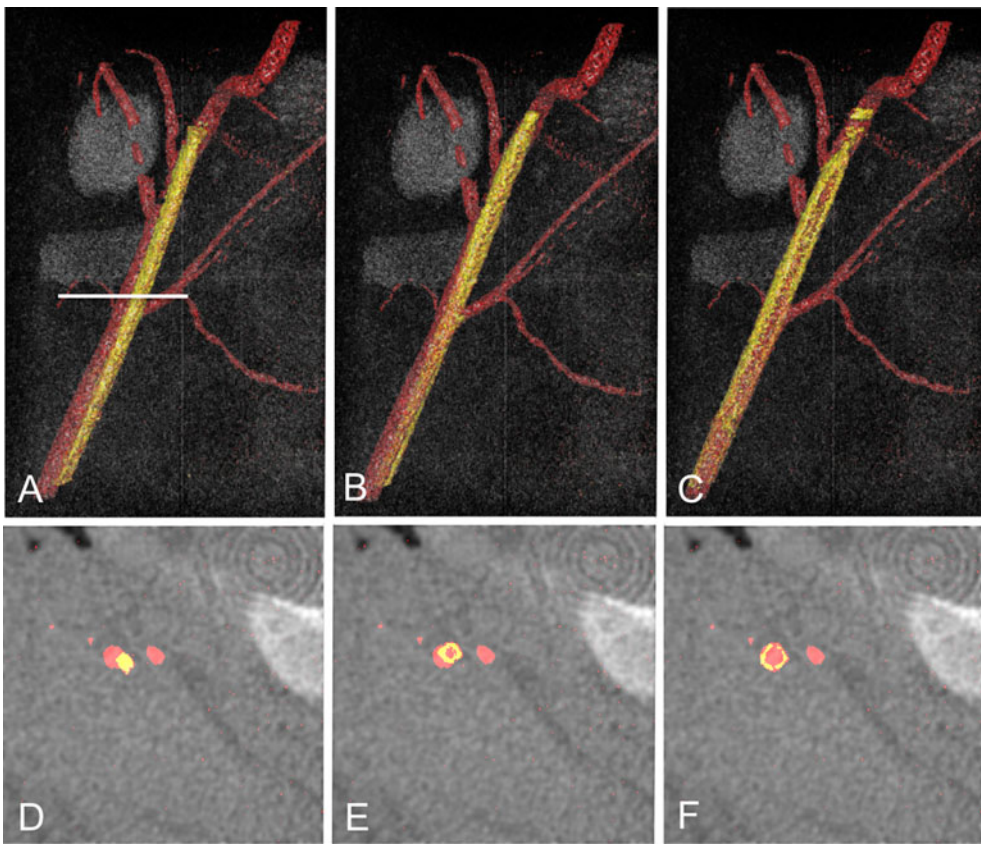

Fig 4 A 4D time-series of an unfolding stent protruding from the common carotid artery of a pig into the external carotid artery. Volume-rendered images in the *upper row* show the unfolding of the stent, beginning in the upper parts of the carotid artery. The *lower row* shows axial images showing the common carotid artery and the stent (slice location is marked by a *white line*). (*See* Supplementary video 2)

after dose reduction. However, the computation time was not optimised because this was a fundamental feasibility study. Real-time reconstruction will require well-designed, parallel reconstruction computer power as well as sophisticated display methods. This is an engineering and programming problem rather than a fundamental problem because current computational power is sufficient [25]. Furthermore, in-depth analysis of image quality as well as imaging parameters and radiation dose should be performed when more concrete set-ups are available.

Four-dimensional imaging requires continuous volumetric data acquisition. A gantry-based continuous rotating imaging chain is currently the most straight-forward platform for this purpose. Such systems seem best suited for neuro-interventions in which direct patient access to the volume examined is not critical. In abdominal interventions, direct access to the imaged area is necessary and open solutions using C-arms might be best suited here. Up-to-date C-arm systems can provide fast rotation speeds, short turnaround times and have flexible positioning systems that could allow complex imaging trajectories, through which 4D guidance might be realised.

The radiation dose rates of gold standard fluoroscopy and 4D interventional guidance using CS image reconstruction in this early prototype implementation are similar and are orders of magnitude lower than that of standard CT fluoroscopy. Air kerma rates of an air chamber that was imaged under realistic guidance conditions for both methods were used as an internal standard in the comparison. This seemed to be the most suitable reference for comparing a 2D technique with a 3D technique and for showing equivalence in terms of applied dose rates. Calculating effective dose rates would have required more assumptions (such as imaged organs, fluoroscopic field of view and imaging direction) which would have resulted in new uncertainties. In no way can air kerma rates reported here be directly compared with published, effective dose rates of intervention guidance.

The information content of both methods is different. It is not straightforward to quantify the advantages of a continuous spatial update over projective imaging. The same holds true for different frame rates and temporal resolutions of both methods. Because of its advantages, 4D intervention guidance may decrease the total time needed for interventions and, therefore, higher dose rates than in 2D fluoroscopy may become acceptable to increase the temporal resolution without increasing the total radiation dose during the procedure. Future developments in data acquisition and reconstruction algorithms may reduce the necessary dose.

Because interventional procedures are rarely performed based on image guidance techniques alone, the total radiation dose of an intervention is the sum of radiation doses from image guidance, angiographies and cone-beam CTs, which are more and more often performed intraprocedurally. In 4D guidance imaging, these could largely be omitted because continuous tomographic information is acquired as needed throughout the procedure, and hence other imaging may be unnecessary.

In conclusion, potential harm through novel technology has to be assessed in relation to potential benefit, as always. Data presented here, and that were based on studies using an early 4D intervention guidance prototype set-up with simulated noise levels, allow to conclude that radiation dose is comparable with the currently accepted norms for interventional procedures. The proposed technique brings considerable advantages by providing 4D images without increasing potential harm. Therefore, future development of this first broadly applicable real-time 4D imaging technique is worthy. The potential for realising improvements in image guidance are great in terms of shorter procedure times, better patient outcomes and the development of new, more complex image-guided procedures.

Acknowledgements The research is funded by DFG (German Research Foundation) grant (KA 1678/6-1 and BA 3546/2-1) and Siemens Healthcare. We acknowledge Stefan Sawall's support in the creation of the reconstruction algorithm and his contribution to the discussion of the methodology. We thank Dr. Michaela Socher and Roland Galmbacher for animal handling. Furthermore, we would like to acknowledge Barbara Flach and Rolf Kueres for help during experimental set-ups and discussion of future developments. We would like to thank Dr. Michael Grasruck, Dr. Andreas Maier and Dr. Yiannis Kyriakou for extensive help with the experimental set-up, as well as discussion of applications, clinical implementation and future developments.

References

1. Rodés-Cabau J (2011) Transcatheter aortic valve implantation: current and future approaches. Nat Rev Cardiol 9:15–29
2. Bock M, Wacker FK (2008) MR-guided intravascular interventions: techniques and applications. J Magn Reson Imaging 27:326–338
3. Schirra CO, Weiss S, Krueger S, Pedersen SF, Razavi R, Schaeffter T, Kozerke S (2009) Toward true 3D visualization of active catheters using compressed sensing. Magn Reson Med 62:341–347
4. Tang J, Hsieh J, Chen G-H (2010) Temporal resolution improvement in cardiac CT using PICCS (TRI-PICCS): performance studies. Med Phys 37:4377–4388
5. Carlson SK, Bender CE, Classic KL, Zink FE, Quam JP, Ward EM, Oberg AL (2001) Benefits and safety of CT fluoroscopy in interventional radiologic procedures. Radiology 219:515–520
6. Racadio JM, Babic D, Homan R, Rampton JW, Patel MN, Racadio JM, Johnson ND (2007) Live 3D guidance in the interventional radiology suite. AJR Am J Roentgenol 189:W357–W364
7. Schulz B, Eichler K, Siebenhandl P, Gruber-Rouh T, Czerny C, Vogl TJ, Zangos S (2012) Accuracy and speed of robotic assisted needle interventions using a modern cone beam computed tomography intervention suite: a phantom study. Eur Radiol 23:198-204
8. Kroeze SGC, Huisman M, Verkooijen HM, van Diest PJ, Ruud Bosch JLH, van den Bosch MAAJ (2012) Real-time 3D fluoroscopy-guided large core needle biopsy of renal masses: a critical early evaluation according to the IDEAL recommendations. Cardiovasc Intervent Radiol 35:680–685

9. Mistretta CA (2011) Sub-nyquist acquisition and constrained reconstruction in time resolved angiography. Med Phys 38:2975–2985
10. Neeman Z, Dromi SA, Sarin S, Wood BJ (2006) CT fluoroscopy shielding: decreases in scattered radiation for the patient and operator. J Vasc Interv Radiol 17:1999–2004
11. Donoho DL (2006) Compressed sensing. IEEE Trans Inf Theory 52:1289–1306
12. Chen G-H, Tang J, Leng S (2008) Prior image constrained compressed sensing (PICCS): a method to accurately reconstruct dynamic CT images from highly undersampled projection data sets. Med Phys 35:660–663
13. Tang J, Nett BE, Chen G-H (2009) Performance comparison between total variation (TV)-based compressed sensing and statistical iterative reconstruction algorithms. Phys Med Biol 54:5781–5804
14. Pan X, Sidky EY, Vannier M (2009) Why do commercial CT scanners still employ traditional, filtered back-projection for image reconstruction? Inverse Probl 25:1230009
15. Ritschl L, Bergner F, Fleischmann C, Kachelriess M (2011) Improved total variation-based CT image reconstruction applied to clinical data. Phys Med Biol 56:1545–1561
16. Chen G-H, Tang J, Nett B, Qi Z, Leng S, Szczykutowicz T (2010) Prior image constrained compressed sensing (PICCS) and applications in X-ray computed tomography. Curr Med Imaging Rev 2:119–134
17. Chen GH, Tang J, Leng S (2008) Prior Image Constrained Compressed SEnsing (PICCS). Proc Soc Photo Opt Instrum Eng 6856:685618
18. Feldkamp LA, Davis LC, Kress JW (1984) Practical cone-beam algorithm. J Opt Soc Am 1:612–619
19. McKinnon GC, Bates RH (1981) Towards imaging the beating heart usefully with a conventional CT scanner. IEEE Trans Biomed Eng 28:123–127
20. Sidky EY, Pan X, Reiser IS, Nishikawa RM, Moore RH, Kopans DB (2009) Enhanced imaging of microcalcifications in digital breast tomosynthesis through improved image-reconstruction algorithms. Med Phys 36:4920–4932
21. Candes EJ, Plan Y (2011) A probabilistic and RIPless theory of compressed sensing. IEEE Trans Inf Theory 57:7235–7254
22. Gupta R, Grasruck M, Suess C, Bartling SH, Schmidt B, Stierstorfer K, Popescu S, Brady T, Flohr T (2006) Ultra-high resolution flat-panel volume CT: fundamental principles, design architecture, and system characterization. Eur Radiol 16:1191–1205
23. Grasruck M, Suess C, Stierstorfer K, Popescu S, Flohr T (2005) Evaluation of image quality and dose on a flat-panel CT-scanner. Proc SPIE 5745:179–188
24. McNitt-Gray MF (2002) AAPM/RSNA physics tutorial for residents: topics in CT. Radiation dose in CT. Radiographics 22:1541–1553
25. Kachelriess M, Knaup M, Bockenbach O (2007) Hyperfast parallel-beam and cone-beam backprojection using the cell general purpose hardware. Med Phys 34:1474–1486